

# Targeted Gene Knockouts Reveal Overlapping Functions of the Five *Physcomitrella patens* FtsZ Isoforms in Chloroplast Division, Chloroplast Shaping, Cell Patterning, Plant Development, and Gravity Sensing

Anja Martin<sup>a</sup>, Daniel Lang<sup>a</sup>, Sebastian T. Hanke<sup>a,b</sup>, Stefanie J.X. Mueller<sup>a,c</sup>, Eric Sarnighausen<sup>a</sup>, Marco Vervliet-Scheebaum<sup>a</sup> and Ralf Reski<sup>a,b,c,1</sup>

<sup>a</sup> Plant Biotechnology, Faculty of Biology, University of Freiburg, Schaenzlestr. 1, 79104 Freiburg, Germany

<sup>b</sup> Centre for Biological Signalling Studies (bioss), University of Freiburg, Alberstr. 19, 79104 Freiburg, Germany

<sup>c</sup> Spemann Graduate School of Biology and Medicine (SGBM), University of Freiburg, Alberstr. 19A, 79104 Freiburg, Germany

**ABSTRACT** Chloroplasts and bacterial cells divide by binary fission. The key protein in this constriction division is FtsZ, a self-assembling GTPase similar to eukaryotic tubulin. In prokaryotes, FtsZ is almost always encoded by a single gene, whereas plants harbor several nuclear-encoded FtsZ homologs. In seed plants, these proteins group in two families and all are exclusively imported into plastids. In contrast, the basal land plant *Physcomitrella patens*, a moss, encodes a third FtsZ family with one member. This protein is dually targeted to the plastids and to the cytosol. Here, we report on the targeted gene disruption of all *ftsZ* genes in *P. patens*. Subsequent analysis of single and double knockout mutants revealed a complex interaction of the different FtsZ isoforms not only in plastid division, but also in chloroplast shaping, cell patterning, plant development, and gravity sensing. These results support the concept of a plastoskeleton and its functional integration into the cytoskeleton, at least in the moss *P. patens*.

**Key words:** Bryophyte; cell wall; gravitropism; GTPase; chloroplast; plastoskeleton; *P. patens*; moss.

## INTRODUCTION

Plants arose from an endosymbiotic event in which a fully differentiated eukaryotic cell engulfed a free-living cyanobacterium, which was subsequently 'domesticated' as a chloroplast (Gould et al., 2008; Gray, 1992). This process was not simply a mere merger of two autonomous cells, but a co-evolutionary process at the cellular level, involving gene transfer (e.g. Martin et al., 1998) and rearrangement of cellular structures (Kuroiwa et al., 2008). Consequently, chloroplasts divide by binary fission as bacterial cells do (Kuroiwa et al., 1998; Possingham and Lawrence, 1983). Both processes rely on the protein FtsZ (filamentous temperature sensitive Z), a self-assembling GTPase that can form a contractile ring at the prospective division site (Dai and Lutkenhaus, 1991; de Boer et al., 1992; Gilson and Beech, 2001; Osteryoung et al., 1998; Osteryoung and Vierling, 1995; Strepp et al., 1998; Yoshida et al., 2006). It is now widely accepted that FtsZ is a prokaryotic homolog of the eukaryotic tubulin (Erickson et al.,

1996; Lowe and Amos, 1998). In the plastid division complex, FtsZ interacts with ARC6, a descendant of a cyanobacterial cell division protein (Vitha et al., 2003), ARC5, a descendant of

<sup>1</sup> To whom correspondence should be addressed at address <sup>a</sup>. E-mail Ralf. Reski@biologie.uni-freiburg.de, fax +49 761-203-6967, tel. +49 761-203-6969.

© The Author 2009. Published by the Molecular Plant Shanghai Editorial Office in association with Oxford University Press on behalf of CSPP and IPPE, SIBS, CAS.

The online version of this article has been published under an open access model. Users are entitled to use, reproduce, disseminate, or display the open access version of this article for non-commercial purposes provided that: the original authorship is properly and fully attributed; the Journal and Oxford University Press are attributed as the original place of publication with the correct citation details given; if an article is subsequently reproduced or disseminated not in its entirety but only in part or as a derivative work this must be clearly indicated. For commercial re-use, please contact journals.permissions@oupjournals.org  
doi: 10.1093/mp/ssp076, Advance Access publication 10 September 2009  
Received 27 May 2009; accepted 7 August 2009

a protein involved in eukaryotic cell division (Miyagishima et al., 2008), and with PDV-proteins, which seem to be specific to land plants (Miyagishima et al., 2006).

While most bacteria encode one single FtsZ protein, plants harbor at least three different nuclear-encoded FtsZ proteins in two small protein families, FtsZ1 and FtsZ2. Phylogenetic analyses revealed that all plant FtsZ proteins can be traced back to their cyanobacterial ancestor and that the split into different families occurred in an ancestor of Viridiplantae (Osteryoung et al., 1998; Rensing et al., 2004). The existence of multiple FtsZ isoforms in a single plant immediately suggests that they may have different functions. In fact, FtsZ1 and FtsZ2 proteins can be discriminated by three features: (1) Plant FtsZ1 proteins share the serine residue found in the tubulin signature, whereas all plant FtsZ2 proteins have a threonine residue also found in bacterial FtsZ (El-Shami et al., 2002). (2) FtsZ2 proteins possess a conserved C-terminal domain, which is absent in FtsZ1 proteins. In bacteria, this domain mediates interaction between FtsZ and other cell division proteins (e.g. Ma and Margolin, 1999). (3) FtsZ1 and FtsZ2 proteins differ in their biochemical properties and *in vivo* localization (El-Kafafi et al., 2005). Evidence for the functional difference of the two families in flowering plants came from studies in *Arabidopsis thaliana*: while overexpression of *AtftsZ1-1* inhibited chloroplast division, slight overexpression of *AtftsZ2-1* did not affect the chloroplast division (Stokes et al., 2000) whereas strong overexpression of this gene impaired plastid division (McAndrew et al., 2001). In addition, antisense lines of both genes exhibited strongly reduced chloroplast numbers per cell (Osteryoung et al., 1998). Furthermore, *AtFtsZ1::GFP* fusion proteins, but not those of the *AtFtsZ2*-family, were found not only in rings, but also in stromules (Vitha et al., 2001), stroma-filled tubules emanating from the chloroplast (Köhler et al., 1997).

Surprisingly, basal land plants encode a third FtsZ family, making the moss *Physcomitrella patens* currently the organism with the most different FtsZ proteins, namely five. This finding prompted us to change the nomenclature of the moss FtsZ isoforms (Martin et al., 2009). While the PpFtsZ2-family was not affected, the former FtsZ1-2 is now referred to as FtsZ3, while the most recently found *ftsZ* gene encodes FtsZ1-2. This new nomenclature is used in the following text and differs from the nomenclature used in previous publications regarding FtsZ1-2 and FtsZ3. Similar to the situation in *A. thaliana*, both *P. patens* FtsZ1-isoforms are localized to rings in chloroplasts and surrounding the plastids and to long filaments in stromules. In addition, both moss FtsZ1-isoforms form filamentous networks inside the chloroplasts (Gremillon et al., 2007; Martin et al., 2009; Suppanz et al., 2007). Both FtsZ2-isoforms of *P. patens* (PpFtsZ2-1, PpFtsZ2-2) are found as network-like structures in the plastids, suggesting that they act as components of a plastoskeleton that may ensure chloroplast shape and integrity (Kiessling et al., 2000; Reski, 2002). Similar to the situation in *A. thaliana*, however, PpFtsZ2 proteins are not found in stromules. The single member of the third

FtsZ-family (PpFtsZ3), which has no ortholog in seed plants, is dually targeted to chloroplasts and to the cytosol in *P. patens*, localizing to ring-like structures in both compartments. As transient overexpression of this gene hampered cell and chloroplast division, it was suggested that this dually targeted protein may represent a molecular link between cell and organelle division in moss (Kiessling et al., 2004). From studies using fluorescence energy transfer (FRET), it became evident that the different FtsZ isoforms specifically and in a hierarchical order interact *in vivo* in plastids and in the cytosol of *P. patens* (Gremillon et al., 2007). It remained elusive, however, what the biological significance of these interactions might be.

In contrast to the situation in *A. thaliana*, the generation of loss-of-function mutants by targeted gene disruption is a straightforward approach in *P. patens* (Reski, 1998a). Consequently, targeted disruption of Pp*ftsZ2-1* proved the importance for FtsZ in chloroplast division (Strepp et al., 1998). It was, however, not clear until the complete genome of *P. patens* was sequenced (Rensing et al., 2008) that this moss encodes not only four, but five different FtsZ proteins (Martin et al., 2009). Here, we report on the creation of a series of FtsZ deletion mutants, including single ( $\Delta$ Pp*ftsZ1-1*,  $\Delta$ Pp*ftsZ1-2*,  $\Delta$ Pp*ftsZ2-1*,  $\Delta$ Pp*ftsZ2-2*, and  $\Delta$ Pp*ftsZ3*), and double mutants ( $\Delta$ Pp*ftsZ1-1/1-2* and  $\Delta$ Pp*ftsZ2-1/2-2*). Their subsequent analysis revealed specific functions of the different FtsZ families, as well as the individual members of each family, not only in chloroplast division, but also in chloroplast shaping and in different cellular processes. These results are discussed from an evolutionary point of view, supporting the concept of a plastoskeleton and its functional integration into the cytoskeleton, at least in the moss *P. patens*.

## RESULTS

### Generation of *ftsZ* Knockout Mutants

The nuclear genome of *P. patens* encodes five different *ftsZ* genes; two closely related paralogs in the FtsZ1 and FtsZ2 family, respectively, and a single member in the basal plant-specific FtsZ3 family (Figure 1; Martin et al., 2009). Targeted gene knockout of *ftsZ2-1* was previously reported and proved the function of the encoded protein in chloroplast division (Strepp et al., 1998).

To unravel the functions of the other four FtsZ proteins, we generated single and double deletion mutants making use of *P. patens*' high rate of homologous recombination in its nuclear DNA. Knockout constructs comprising genomic *ftsZ* fragments interrupted by a selection cassette that confers resistance to either hygromycin or G418 were generated for *ftsZ1-1*, *ftsZ1-2*, *ftsZ3*, and *ftsZ2-2* (Figure 2A and 2B). The constructs were introduced into *P. patens* employing PEG-mediated transformation of isolated protoplasts. Several independent single and double knockout mutants were identified (see Table 1 for an overview).

All plants were initially screened via direct PCR (Schween et al., 2002) for disruption of the wild-type *ftsZ* locus as well as correct 5' and 3' integration of the construct with primers

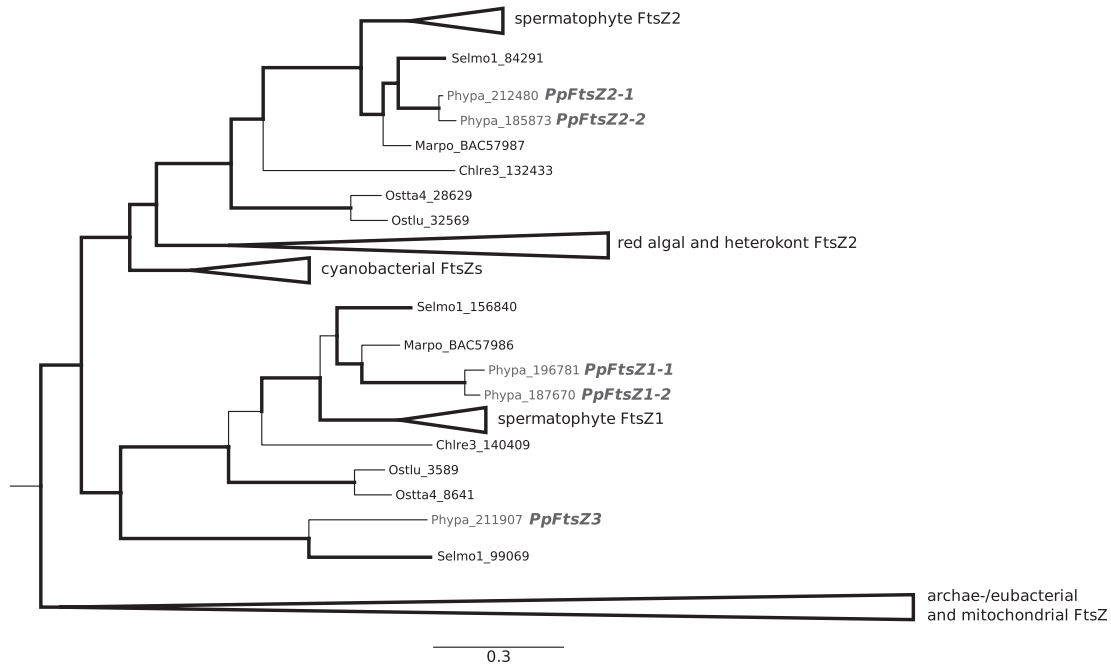


**Figure 1.** Phylogenetic Relationships of the Eukaryotic FtsZ Family with a Special Focus on the Gene Family in *Physcomitrella patens* (Adapted from Tree Described in Martin et al., 2009).

Branch thickness indicates branch support as posterior probabilities. *Physcomitrella* FtsZ proteins are highlighted in gray. The tree is rooted using the archaeal/eubacterial and mitochondrial FtsZs clade as outgroup (shown collapsed). To focus on phylogenetic relationships of the moss gene family, branches of the seed plant (Spermatophyta), red algal (Rhodophyta), and heterokont algal (stramenopiles) FtsZ subfamilies have been collapsed as well. Selmo, *Selaginella moellendorffii* (Lycopodiophyta); Marpo, *Marchantia polymorpha* (Marchantiophyta); Chlre, *Chlamydomonas reinhardtii* (Chlorophyta); Ostta, *Ostreococcus tauri* (Prasinophyceae); Ostlu, *Ostreococcus lucimarinus* (Prasinophyceae).

that bind outside of the introduced construct and inside the selection cassette (Figure 2C and Supplemental Figure 1). From plants with positive results after direct PCR screening, protonema was grown in liquid cultures to obtain larger amounts of plant material for RNA isolation and subsequent RT-PCR analysis (Figure 2D–2G and 2I–2J). For putative  $\Delta ftsZ2-2$ , an additional Northern blot was performed due to the presence of faint traces of transcript after RT-PCR that was most probably caused by unspecific binding of the primers to *ftsZ2-1* (Figure 2H). The confirmed deletion mutants were grown under standard conditions and subsequently compared to wild-type.

#### Phenotypic Analyses of $\Delta ftsZ1$ Mutants

The overall plant morphology of  $\Delta ftsZ1-1$ ,  $\Delta ftsZ1-2$ , and  $\Delta ftsZ1-1/1-2$  mutants did not differ from *P. patens* wild-type. Likewise, plant growth and development were not obviously different from the control. To investigate a possible involvement of *P. patens* FtsZ1 proteins in plastid division, chloroplast shape and numbers were compared between the deletion mutants and wild-type. In the latter chloronema cells harbored about 50 lens-shaped chloroplasts (Figure 3A). Interestingly,  $\Delta ftsZ1-1$  mutants did not show altered chloroplast morphology or number (Figure 3B), while  $\Delta ftsZ1-2$  mutants had enlarged plastids only in basal chloronema cells (Figure 3C). In contrast, the  $\Delta ftsZ1-1/1-2$  double mutants displayed chlor-

oplasts with drastically altered shapes in every cell and tissue type. In these mutants, chloroplasts were enlarged and elongated, with pointed poles. Most chloronema cells of these double gene knockout mutants contained three to five chloroplasts per cell only (Figure 3D). When compared to wild-type, the gametophores of these mutants appeared to be smaller (Figure 3H).

#### Phenotypic Analyses of $\Delta ftsZ2$ Mutants

Re-examination of the previously published  $\Delta ftsZ2-1$  mutants (Strepp et al., 1998) confirmed that they contained only one to three giant chloroplasts per cell (Figure 3E). In contrast, targeted deletion of the *ftsZ2-2* gene did not obviously affect shape or number of the plastids (Figure 3F). In contrast, the  $\Delta ftsZ2-1/2-2$  double mutants harbored one to three macrochloroplasts in every cell (Figure 3G). Gametophores of these mutants were obviously shorter than in the wild-type (Figure 3H). In addition, the double mutant displayed altered leaf morphology, including irregular cell patterning throughout the leaves. While cells in leaves of wild-type, of  $\Delta ftsZ2-1$  mutants, and of  $\Delta ftsZ2-2$  mutants were regularly arranged in parallel to the midrib and possessed an approximately rectangular shape, cell shapes in the  $\Delta ftsZ2-1/2-2$  double mutants were highly diverse, the leaves having also a distorted midrib and a disturbed cell arrangement (Figure 3I and 3J).

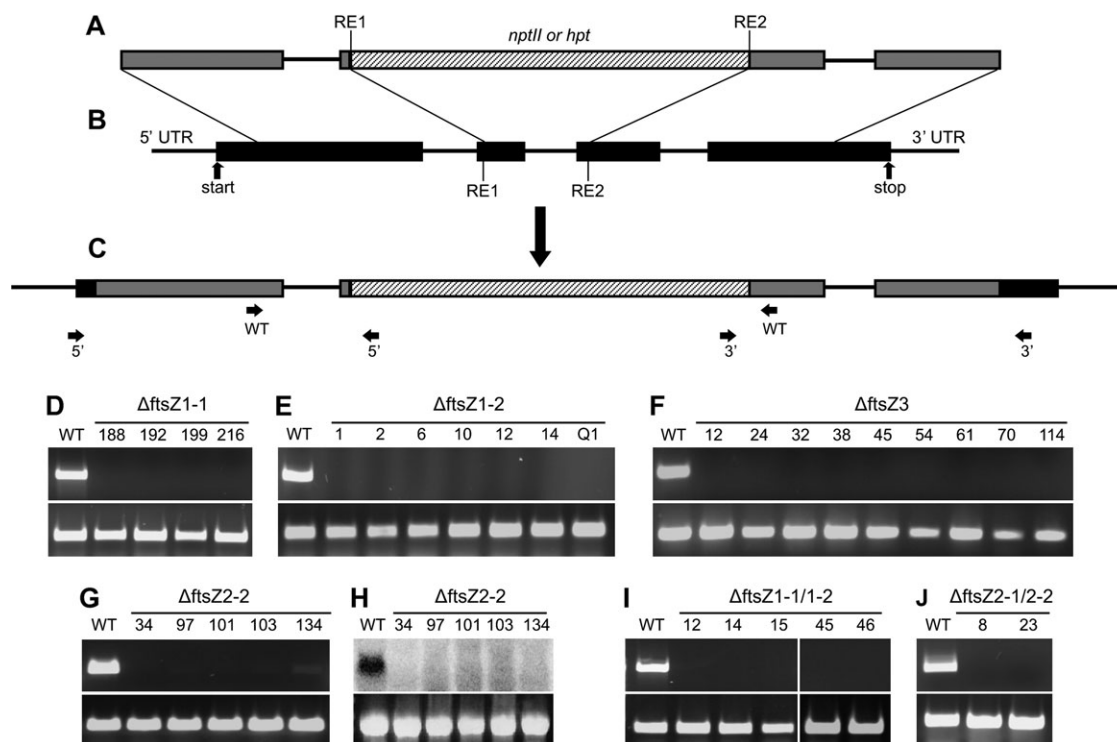


**Figure 2.** Generation and Molecular Analysis of *P. patens*  $\Delta$ *ftsZ* Mutants.

(A) Exemplary scheme of the generated knockout constructs (RE: restriction enzyme).

(B) The genomic locus.

(C) The altered structure of the genomic locus after integration of the knockout construct by homologous recombination. Primer pairs that were used for direct PCR plant screening are indicated as arrows and are listed in Table 3 for the *ftsZ* knockouts.

(D–G, I–J) RT-PCR analysis with gene-specific primers (see Table 4). As a control, RT-PCR was performed with primers C45fwd and C45rev, corresponding to the constitutively expressed gene for the ribosomal protein L21. The corresponding PCR-product is always shown in the lower panels.

(H) In addition to RT-PCR, Northern blot analysis was performed for putative  $\Delta$ *ftsZ2-2* mutants due to the presence of faint traces of transcript after RT-PCR. As a control for equal loading of RNA ethidium bromide stained 28S rRNA is shown (lower panel).

**Table 1.** After Three Rounds of Selection on Medium Containing Antibiotics, Transgenic Plants Were Analyzed Via Direct PCR.

	$\Delta$ <i>ftsZ1-1</i>	$\Delta$ <i>ftsZ1-2</i>	$\Delta$ <i>ftsZ3</i>	$\Delta$ <i>ftsZ2-2</i>	$\Delta$ <i>ftsZ1-1/1-2</i>	$\Delta$ <i>ftsZ2-1/2-2</i>
Direct PCR	180	132	238	34	46	192
Correct 5' and 3' integration	22*	19*	9	5	11*	2
Absence of WT transcript	4	7	9	5	5	2

All plants with correct 5' and 3' integration of the knockout construct into the respective locus were further tested for absence of the *ftsZ* transcript via RT-PCR. \* RNA for subsequent RT-PCR analysis was extracted from only a subset of the plants.

### Phenotypic Analyses of $\Delta$ *ftsZ3* Mutants

Targeted knockout of the *ftsZ3* gene severely affected overall plant morphology. The leafy gametophores (the adult gametophytes) of  $\Delta$ *ftsZ3* mutants were shorter, stunted, and more compact than those of wild-type (Figure 4A). The leaf cells of these mutants harbored a variety of unusual chloroplast num-

bers and shapes. In different cells of a single leaf, macrochloroplasts, enlarged plastids with finger-like outgrowths, and other irregularly shaped chloroplasts were observed (Figure 4B). The  $\Delta$ *ftsZ3* mutants also displayed severe perturbations of leaf cell pattern while the overall shape of the leaves was only moderately altered when compared to wild-type (Figures 4C). Under standard growth conditions, the average length of wild-type gametophores was 3.3 mm, while mutant gametophores were reduced to 2.1–2.5 mm in length (Figure 4D and 4E). Further, deletion of the *ftsZ3* gene resulted in reduced lengths of the leaves themselves. While in wild-type, the average leaf was 1.2 mm long, the leaves of the deletion mutants were reduced to 0.8–1.1 mm in length (Figure 4D and 4E). In contrast, the gene deletion did not obviously affect the leaf width (Figure 4E).

Light microscopy of the filamentous protonema tissues revealed highly unusual plastid morphologies in the  $\Delta$ *ftsZ3* mutants: chloroplasts appeared as strongly enlarged or elongated, tubular, and rather thin structures (Figure 5A). However, transmission electron micrographs (TEM) showed that deletion of the *ftsZ3* gene did not affect the internal fine

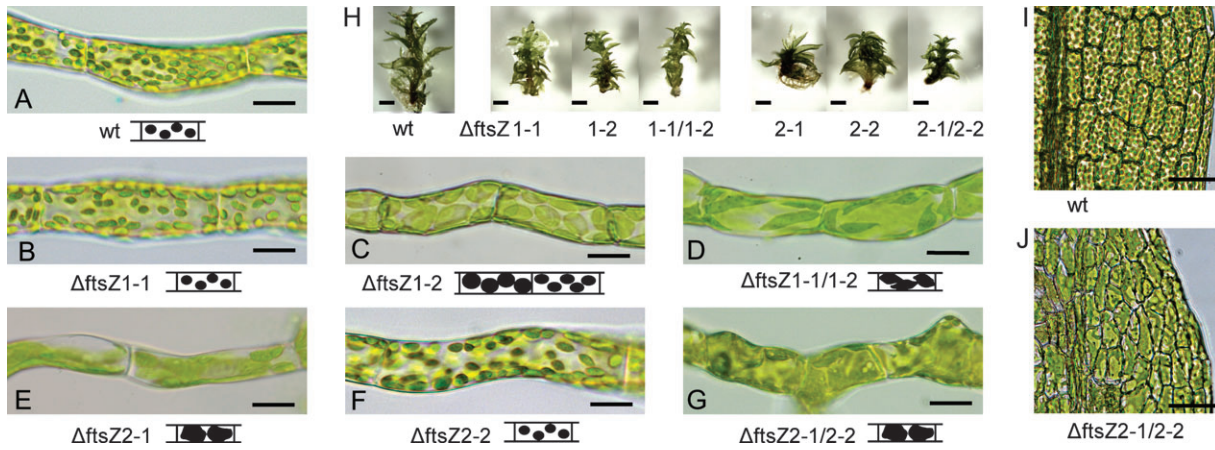


**Figure 3.** Knockout of *ftsZ1* and *ftsZ2* Genes Affects Chloroplast Morphology. Protonema cells of (A) WT, (B)  $\Delta$ *ftsZ1-1*, (C)  $\Delta$ *ftsZ1-2*, (D)  $\Delta$ *ftsZ1-1/1-2*, (E)  $\Delta$ *ftsZ2-1*, (F)  $\Delta$ *ftsZ2-2*, and (G)  $\Delta$ *ftsZ2-1/2-2* mutants (scale bar = 25  $\mu$ m). (H) Gametophores of WT and of *ftsZ1* and *ftsZ2* mutants (scale bar = 250  $\mu$ m). Sector of a leaf of (I) WT and (J)  $\Delta$ *ftsZ2-1/2-2* mutant (scale bar = 50  $\mu$ m).

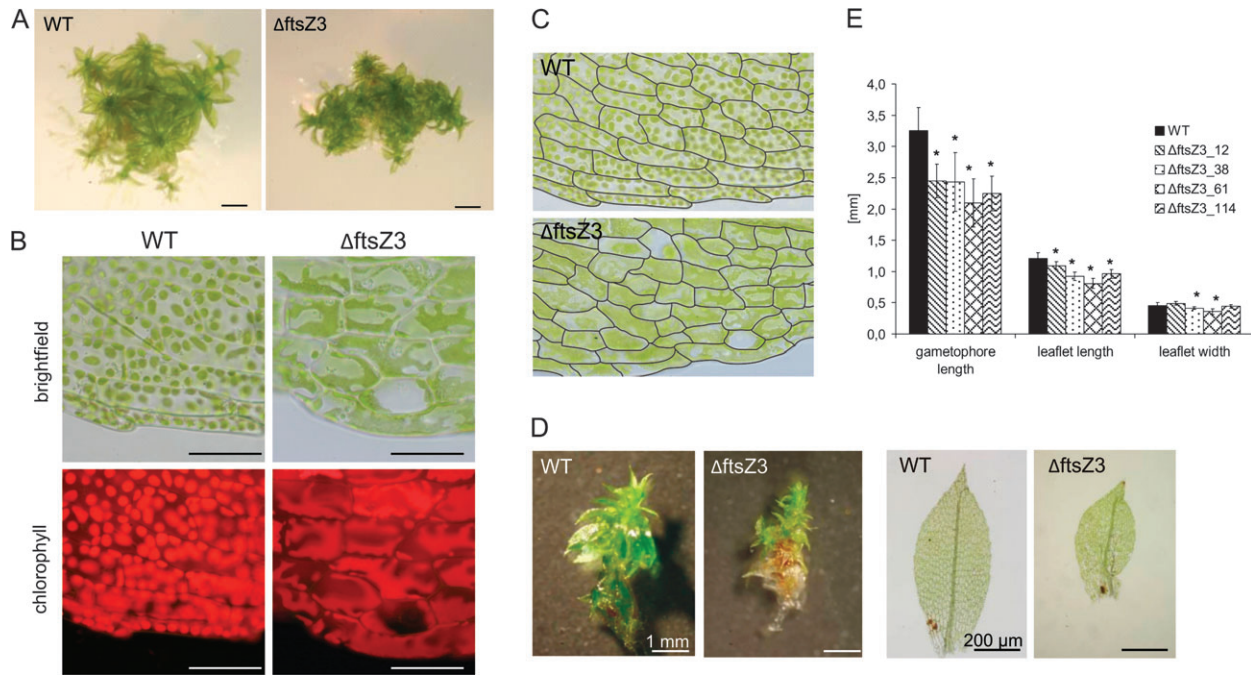


**Figure 4.** Knockout of *ftsZ3* Affects Plant and Chloroplast Morphology. (A) Wild-type and *ftsZ3* gametophyte (scale bars = 1 mm). (B) Micrographs of leaf cells of the wild-type and  $\Delta$ *ftsZ3* (scale bar = 50  $\mu$ m) under brightfield and UV-fluorescence. (C) Cell patterning in leaf cells of WT (upper panel) and  $\Delta$ *ftsZ3* (lower panel). Cell walls were traced using graphical software. (D) Stereo and light microscope images of gametophores and leaves from WT and  $\Delta$ *ftsZ3* grown in parallel under standard conditions for 4 weeks. (E) Measurement of gametophore and leaf dimensions. Columns represent the average length of gametophores ( $n = 14$ ) and length and width of leaves ( $n = 20$ ) grown on Knop medium for 4 weeks. Error bars indicate the absolute average deviation (AAD). Asterisks indicate significant differences between WT and  $\Delta$ *ftsZ3* ( $t$ -test,  $P \leq 0.001$ ).

structure of the chloroplasts. Surprisingly, cell walls of the mutant were obviously thinner as compared to cell walls of wild-type *P. patens* (Figure 5B). Subsequently, we measured cell wall thickness at three different positions per thin section. These

measurements revealed that cell walls of wild-type were, on average, 263 nm thick, whereas the cell walls in  $\Delta$ *ftsZ3* mutants were reduced to about one-third (90 nm). This difference in cell wall thickness was significant, with  $P \leq 0.001$  (Figure 5C). In

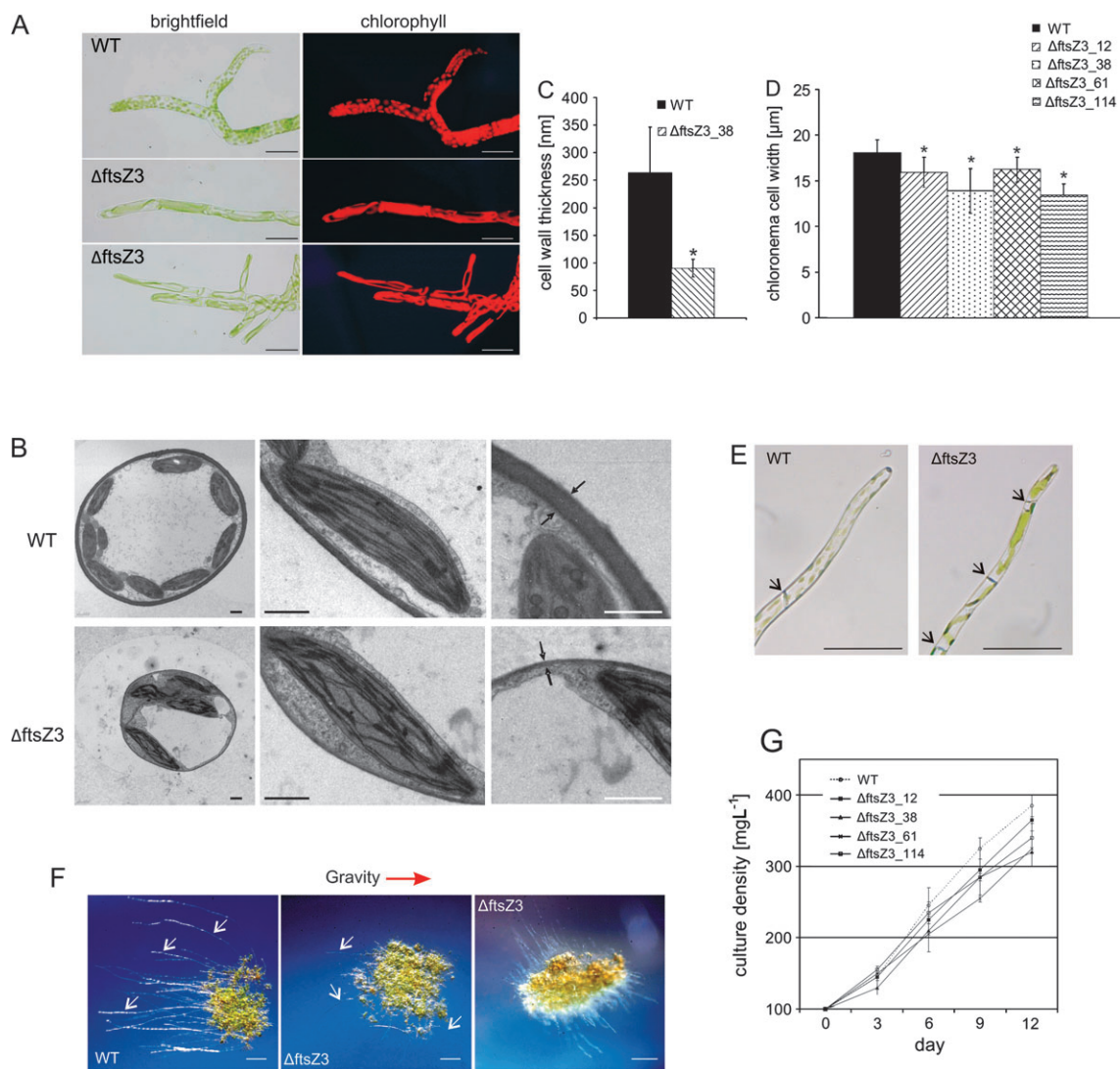


**Figure 5.** Wide Range of Phenotypic Aberrations in  $\Delta$ ftsZ3 Mutants.

(A) Micrographs of chloronema cells of the wild-type and  $\Delta$ ftsZ3 (scale bar = 50  $\mu$ m).

(B) TEM images of protonema cell cross-sections as well as magnified images of chloroplasts and cell walls are shown. Cell walls are indicated by arrows (scale bar = 1  $\mu$ m).

(C) Mean cell wall thickness for WT and  $\Delta$ ftsZ3. Cell walls from protonema cells, embedded for TEM analysis 4 d after sub-culturing, were measured (WT:  $n = 21$ ; KO:  $n = 24$ ). Asterisks indicate significant differences between WT and mutant ( $t$ -test,  $P \leq 0.001$ ). Error bars indicate the AAD.

(D) Mean width of chloronema cells 4 d after sub-culturing. Asterisks indicate significant differences between WT and mutants ( $t$ -test,  $P \leq 0.001$ ). Error bars indicate the AAD ( $n = 71$ ).

(E) Caulonema cells of WT and  $\Delta$ ftsZ3. Black arrows indicate the position of the cell walls (scale bar = 50  $\mu$ m).

(F) Comparison of caulonema development in the dark between WT and  $\Delta$ ftsZ3. Stereomicroscope images of protonema colonies, grown in the dark on Knop medium. Caulonema filaments are pointed out by white arrows. The gravity vector is indicated by a red arrow (scale bar = 1 mm).

(G) Biomass accumulation of WT and  $\Delta$ ftsZ3 mutants. Biomass accumulation is displayed as the culture density increasing over time. Liquid cultures were inoculated with 100  $\text{mg L}^{-1}$  dry weight (day 0) and growth was monitored for a period of 12 d. Error bars indicate the AAD ( $n = 2$ ).

addition, chloronema cells of  $\Delta$ ftsZ3 mutants were significantly ( $P \leq 0.001$ ) thinner than those of wild-type (Figure 5D).

In wild-type *P. patens*, chloronema cells were cylindrically shaped, with their cross walls perpendicularly orientated with

respect to the growth axis. They contained approximately 50 chloroplasts per cell. In the course of normal development, cell differentiation to another cell type, the caulonema, occurred. These caulonema cells originated from chloronema cells and

were longer and thinner, with cross walls orientated obliquely to the growth axis. These caulonema cells harbored, on average, 19 chloroplasts, which were smaller than those found in chloronema cells (Figure 5E). Under standard growth conditions,  $\Delta ftsZ3$  mutants did hardly develop any caulonema cells. Moreover, those few did not show wild-type characteristics (Figure 5E). As it has been reported that the addition of the phytohormone auxin (Decker et al., 2006), as well as growth in the dark (Vandenbussche et al., 2007), induces caulonema formation in *P. patens*, both treatments were applied separately in this study as well. In accordance with previous findings, wild-type *P. patens* showed numerous long, negatively gravitropic growing caulonema filaments under inductive conditions. The same conditions induced some caulonema filaments in the  $\Delta ftsZ3$  mutants. These, however, were much shorter and less numerous than in wild-type and, furthermore, had lost their gravitropic response, as they grew in different directions (Figure 5F). In addition to that, a comparison of biomass accumulation in wild-type and  $\Delta ftsZ3$  mutants, both inoculated with equal amounts of protonema, revealed growth retardation of the  $\Delta ftsZ3$  mutants (Figure 5G).

#### FtsZ Transcript Levels in Wild-Type and *ftsZ* Deletion Mutants

Our previous studies revealed a complex, well ordered network of FtsZ protein–protein interactions in *P. patens* (Gremillon et al., 2007). Partial redundancy and co-regulatory effects between *ftsZ* genes in *P. patens* have been discussed but not studied at the transcript level by quantitative real-time PCR (qRT–PCR), so far. To this end, measurements of transcript levels from wild-type *P. patens* and the deletion mutants cultured as protonema under standard conditions for 2 weeks were performed. Dry weights of the cultures were adjusted to 150 mg L<sup>-1</sup> each and the cultures were harvested 3 d after the last sub-cultivation at the same time of day. In addition to the five *ftsZ* genes, transcript abundances of the two constitutively expressed genes *l21* and *ef1 $\alpha$*  were analyzed. Use of two reference genes and their mean Cp values for normalization enhanced reliability of qRT–PCR results according to Vandesompele et al. (2002). All transcript levels were measured and compared using ANOVA. Tukey's Honestly Significant Differences (HSD) was used to evaluate potentially significant differences in gene expression (The R Development Core Team, 2009).

In wild-type *P. patens*, we found significantly more *ftsZ1-2* transcripts than *ftsZ1-1* transcripts. Likewise, transcript abundances for *ftsZ2-1* were significantly higher than for *ftsZ2-2* (Figure 6A). Targeted deletion of one or two *ftsZ* genes affected transcript abundances of the others when compared to wild-type (Figure 6B–6D). Remarkably, transcript levels of *ftsZ1-1* were increased when a gene of the *ftsZ2* or *ftsZ3* family was deleted, whereas deletion of the *ftsZ1-2* gene did not affect *ftsZ1-1* transcript abundance. Similarly, transcript abundances of *ftsZ2-1* were most affected by deletion of any of the *ftsZ1* genes, but nearly not by deletion of *ftsZ2-2*. However,

deletion of the *ftsZ1* genes led to reduced transcript levels of *ftsZ2-1*. In addition, deletion of *ftsZ1-2* and of *ftsZ2-1*, respectively, led to reduced transcript levels of *ftsZ3* (Figure 6B–6D).

## DISCUSSION

The genome of the moss *P. patens* encodes five *ftsZ* genes that are members of three distinct subfamilies (Martin et al., 2009). For flowering plants, only genes belonging to two of the *ftsZ* subfamilies have been found (Osteryoung et al., 1998). To investigate the function of those five moss *ftsZ* genes, single knockout mutants of all *P. patens* *ftsZ* genes and double knockout mutants for the *ftsZ1* and *ftsZ2* gene families were generated. Since it is puzzling in an evolutionary sense that the morphologically less complex bryophyte *P. patens* possesses an expanded complement of *ftsZ* genes as compared to flowering plants, our aim was also to identify functional differences to the previously published *A. thaliana* FtsZ proteins.

#### Possible Functions of FtsZ1 Proteins in *P. patens*

The *P. patens* proteins FtsZ1-1 and FtsZ1-2 share high sequence identity and are considered as paleologs (Martin et al., 2009), namely they were derived from an ancient large-scale duplication event along the lineage leading to *Physcomitrella* (Rensing et al., 2007). The targeted deletion of *ftsZ1-1* did not lead to an aberrant chloroplast phenotype whereas  $\Delta ftsZ1-2$  mutants possess enlarged plastids in basal zones of chloronema filaments. In contrast to the lens-shaped wild-type-like plastids observed in the single knockouts,  $\Delta ftsZ1-1/1-2$  double mutants showed altered plastid shape and size in every cell and tissue type. These findings suggest that PpFtsZ1-1 in interaction with PpFtsZ1-2 fulfils functions related to the maintenance of chloroplast shape. This function could be partially accomplished by FtsZ1-2 in the  $\Delta ftsZ1-1$  mutants so that loss of the FtsZ1-1 protein did not have visible effects on moss plants. Such partial redundancy between two FtsZ proteins of the same subfamily was previously reported for the FtsZ2 proteins in *A. thaliana* (McAndrew et al., 2008). From previous studies by Gremillon et al. (2007), it is known that PpFtsZ1-1 is localized to network structures inside the chloroplast and that it participates in the formation of the plastid division apparatus, thus being involved in chloroplast division.

The observed enlargement of chloroplasts in basal chloronema cells of  $\Delta ftsZ1-2$  mutants revealed a role for PpFtsZ1 in controlling the size of plastids. Localization studies employing an *ftsZ1-2:gfp* fusion visualized the protein in network structures within the plastids and as a ring surrounding the middle of the organelle (Martin et al., 2009). This ring might exert force on the chloroplast during the plastid division process. It could be shown for bacterial FtsZ that this protein is capable by itself and without the use of any interaction partner to generate a force that is sufficient to constrict liposomes (Osawa et al., 2008). Recently, also a mathematical model

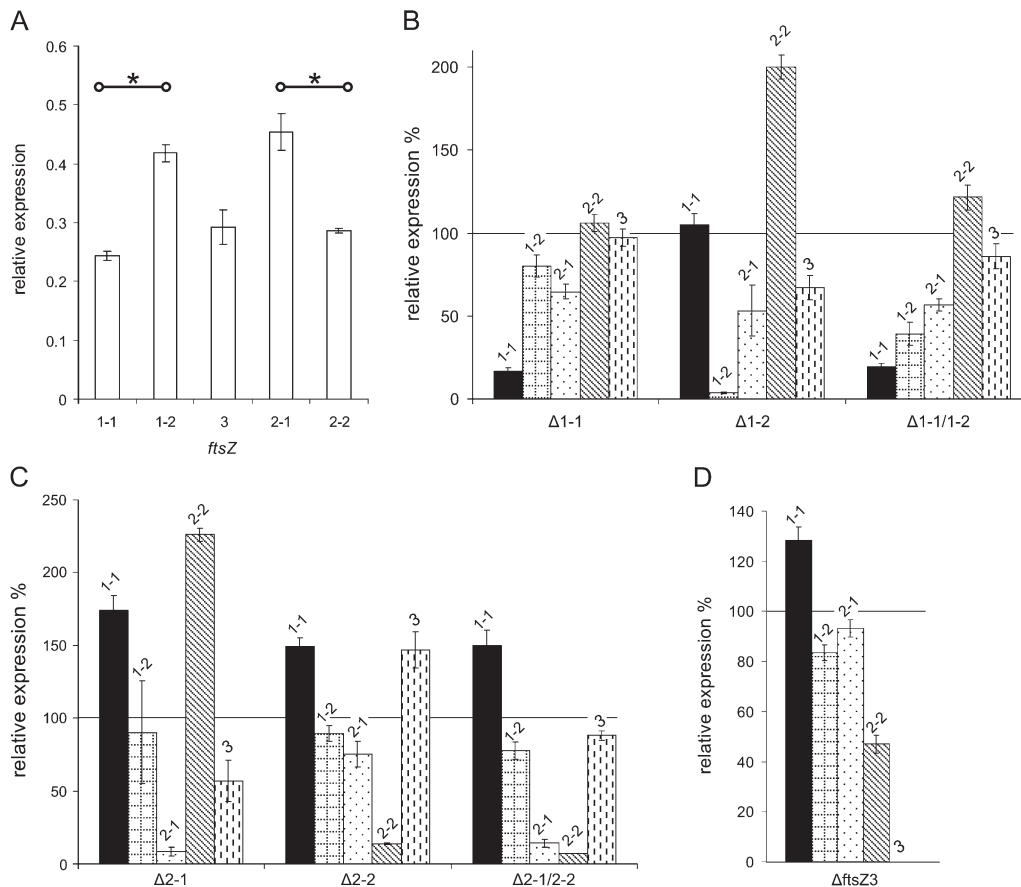


**Figure 6.** FtsZ Transcript Abundance in Wild-Type and in *ftsZ* Single and Double Knockout Mutants.

**(A)** Relative expression level of all five *ftsZ* genes in wild-type. Asterisks indicate significant differences (ANOVA, Tukeys HSD,  $P < 0.001$ ) between two members of the same family.

**(B–D)** Wild-type is set to 100% (black line) to depict relative expression levels of the single *ftsZ* in the mutants. The graphs are grouped by gene family: (B) FtsZ1, (C) FtsZ2, and (D) FtsZ3. Error bars indicate the standard deviation ( $n = 3$ ). Significant changes in transcript abundance in the wild-type ( $t$ -test,  $P < 0.001$ ) are indicated by an asterisk.

describing the FtsZ constriction forces responsible for *E. coli* cell division has been published (Allard and Cytrynbaum, 2009). Several explanations might account for the enlargement of chloroplasts observed in basal cells of  $\Delta ftsZ1-2$  protonema filaments but not in younger cells/tip cells. Auxin gradients in *P. patens* protonema with highest auxin concentration in the tip cell and decreasing auxin levels in the basal cells have been reported previously (Bierfreund et al., 2003). Auxin, like gibberellins and brassinolides, promote preferential cell growth along the longitudinal axis, while other hormones induce expansion along the traverse axis (Shibaoka and Nagai, 1994). Both protonemal cell types, chloronema and caulonema, expand by tip growth (Menand et al., 2007), which is accompanied by substantial changes in the cytoskeleton (Cole and Fowler, 2006; Hussey et al., 2006; Smith and Oppenheimer, 2005). The resulting physiological, biochemical, and structural gradients from dividing apical cells to non-dividing basal filament cells probably influence the formation of complexes between FtsZ and other interaction partners.

In contrast to *P. patens*, the *A. thaliana* genome encodes only one FtsZ1 protein. Expression inhibition of *AtftsZ1-1* reduced the number of chloroplasts in leaf cells (Osteryoung et al., 1998) while overproduction of the protein led to the formation of either strongly enlarged or long, narrow chloroplasts (Stokes et al., 2000). These observations led to the assumption that *AtFtsZ1-1* is involved in chloroplast division. Based on the data obtained for both *PpftsZ1* single knockout mutants, both proteins have slightly different functions, but together are needed for chloroplast division. It would be intriguing to analyze plants with a different subset of FtsZ1 proteins, like *Nicotiana tabacum*, which encodes four FtsZ1 proteins. So far, it was shown that overexpression of *NtftsZ1-2* led to the formation of only one to three chloroplasts per mesophyll cell (Jeong et al., 2002).

To date, it is unknown whether, in plants, FtsZ protein amounts correlate to their transcript levels. Here, we found much higher *ftsZ1-2* transcript levels compared to *ftsZ1-1* transcript levels. If the ratio of transcripts reflects the protein level ratio, a disruption of *ftsZ1-2* will unbalance the FtsZ pools to

a much larger extent than the disruption of *ftsZ1-1*, and thus would explain the more severe phenotype of the  $\Delta$ *ftsZ1-2* mutants observed in this study. A similar effect of FtsZ pool sizes on the phenotype has been postulated based on the phenotypes of *AtftsZ2-1* mutants (McAndrew et al., 2008). In *P. patens*, targeted deletion of either *ftsZ2* genes or the *ftsZ3* gene led to increased levels of preferentially the *ftsZ1-1* gene, which might reflect a central position of the FtsZ1-1 protein in the protein–protein interaction network.

### Possible Functions of FtsZ2 in *P. patens*

Our re-examination of the  $\Delta$ *ftsZ2-1* phenotype confirmed the conclusions from Strepp et al. (1998) that FtsZ2-1 is important for chloroplast division in all gametophytic cells of *P. patens*. In contrast, targeted deletion of the *ftsZ2-2* gene in the present study did not obviously affect chloroplast shape or division. As with the *ftsZ1* genes, the double deletion of both *ftsZ2* genes gave synergistic effects: the  $\Delta$ *ftsZ2-1/2-2* mutants did not only show macrochloroplasts, as described for  $\Delta$ *ftsZ2-1*, but also had defects not obviously related to chloroplasts, namely aberrant leaf morphology and aberrant cell patterning in the leaves.

Both proteins, FtsZ2-1 and FtsZ2-2, were found in network-like structures in the chloroplast, suggesting that besides a cytoskeleton, a plastoskeleton may exist that helps to maintain plastid shape and integrity (Kiessling et al., 2000). We here found that FtsZ2-2 function in the chloroplast can be substituted by FtsZ2-1. The inability of FtsZ2-2—despite the high sequence similarity of the two proteins—to compensate for loss of FtsZ2-1 might be due to proteins that specifically interact with FtsZ2-1 and that are necessary for the maintenance of plastid integrity. Alternatively, FtsZ2-2 cannot compensate for loss of FtsZ2-1 because the *ftsZ2-1* gene is more highly expressed (Figure 6). The  $\Delta$ *AtftsZ2-2* mutant showed a relatively mild phenotype in comparison to  $\Delta$ *AtftsZ2-1*, although both proteins were reported to have biochemically equivalent functions within the FtsZ2 pool (McAndrew et al., 2008). Hence, partial redundancy in the function of both FtsZ2 proteins seems to exist in *P. patens* and in *A. thaliana*. However, a network structure comparable to the plastoskeleton built by FtsZ2-1 and FtsZ2-2 in *P. patens* has not been described for *A. thaliana*.

As previously shown for the FtsZ1 family, knockout of the *ftsZ2* gene with the highest expression level (*ftsZ2-1*) resulted in the more dramatic phenotypic aberrations, probably as a result of more dramatic changes in the FtsZ2 protein pools. Nevertheless, cellular defects after double knockout of both *ftsZ2* genes were at first glance surprising, as these defects were not seen with other moss mutants with giant chloroplasts, such as in the  $\Delta$ *ftsZ2-1* mutants. As plant FtsZ2 and FtsZ3 proteins have a C-terminal motif facilitating protein–protein interactions (Maple et al., 2005; Martin et al., 2009) like bacterial FtsZ have (Haney et al., 2001; Ma and Margolin, 1999; Yan et al., 2000), it seems plausible that depletion of both PpFtsZ2 isoforms in the double mutants affected interaction networks necessary for

proper cytosolic functions. The most obvious explanation is a disturbed interaction with PpFtsZ3, which is dually targeted to plastids and to the cytosol in *P. patens* (Kiessling et al., 2004), and which is interacting with PpFtsZ2-2 in wild-type moss (Gremillon et al., 2007). Consequently, transcript levels of *ftsZ2-2* are reduced in the  $\Delta$ *ftsZ3* mutants, but not in the other knockout mutants created here.

### Possible Functions of FtsZ3 in *P. patens*

It was previously shown that expression of *ftsZ3:gfp* labeled plastidic as well as cytosolic rings in *P. patens* protoplasts, protonema cells, and leaf cells, indicating that this protein may be a molecular link between cell and chloroplast division in moss (Kiessling et al., 2004).

The  $\Delta$ *ftsZ3* mutants presented here possess giant chloroplasts with unusual shapes different from those observed in knockout mutants of the other *ftsZ* genes. However, especially the tubular macrochloroplasts in protonema cells matched the filamentous growth phenotype of *E. coli* *ftsZ* mutants (Dai and Lutkenhaus, 1991) very well, demonstrating its function in chloroplast division. Unable to divide, the chloroplasts were growing to enormous lengths and the presence of the other four FtsZ proteins prevented them, in accordance with their function in a plastoskeleton, from ballooning up.

In addition, and in accordance with the dual localization of FtsZ3 in moss,  $\Delta$ *ftsZ3* mutants showed numerous phenotypic aberrations, such as retarded plant growth and development, decreased cell wall thickness, altered cell size and shape, and an impaired gravitropic response.

In contrast to our knowledge on cell patterning in *A. thaliana* epidermal tissue (Larkin et al., 2003), the analysis of cell patterning in moss leaves is just beginning (Harrison et al., 2009). The cellular defects observed here, however, reveal a role of cytosolic FtsZ3 in cell patterning of *Physcomitrella*. It remains to be elucidated whether PpFtsZ3 interacts with components of the cytoskeleton or is directly involved in cell shaping analogous to the involvement of bacterial FtsZ in *Caulobacter crescentus* where an FtsZ-dependent mode of peptidoglycan synthesis for cell elongation exists (Aaron et al., 2007). Interestingly, *P. patens* encodes nine homologs of genes related to the bacterial peptidoglycan synthesis pathway, while *A. thaliana* encodes only five of them (Machida et al., 2006). Subsequent analyses of some of these genes revealed their functional differences between cyanobacteria, *P. patens*, and *A. thaliana* (Garcia et al., 2008), revealing evolutionary differences of these genes during land plant evolution, nicely explaining why  $\beta$ -lactam antibiotics inhibit division of bacteria and moss chloroplasts, but not the division of plastids in seed plants (Kasten and Reski, 1997; Reski, 2009). Another evidence for the ancient function of PpFtsZ3 came from Gremillon et al. (2007), who reported that *E. coli* FtsZ can substitute PpFtsZ3 in its protein–protein interaction with PpFtsZ2-2 in *P. patens* cells.

Another striking feature of  $\Delta$ *ftsZ3* mutants is their dramatically decreased cell wall thickness, which points to a disturbed transport of building materials (cellulose, hemicelluloses, and

pectins) to the cell wall. It is known that cellulose is synthesized at the plasma membrane and that its deposition is guided by cortical microtubules (Paredes et al., 2006). Hemicellulose and pectins are synthesized in the Golgi apparatus and reach the growing cell wall via vesicle transport, which is based on actin filaments (Chen et al., 2007). Thus, the cytoskeleton is crucial for cell wall assembly in plants. Similarly, however, FtsZ in physical interaction with MreB, the prokaryotic actin homolog, directs the insertion of new peptidoglycans into the side walls near the growing poles of *E. coli* (Varma et al., 2007). To date, it is unclear whether PpFtsZ3 itself, or via interaction with the cytoskeleton, is facilitating cell wall formation in *P. patens*.

Both cell types of the moss protonema, chloronema and caulonema, grow via tip growth, like pollen tubes of seed plants. While chloronema does not grow in the dark, caulonema grows negatively gravitropic in the absence of light (Cove, 1992). Surprisingly, protonema of  $\Delta ftsZ3$  mutants seemed to consist of chloronema only. In the dark, however, caulonema started to develop, but, unlike the situation in wild-type, these cells did not follow the gravity vector. Moreover, the cross walls in the mutants did not show the oblique orientation that in wild-type moss is mediated by microtubules (Reski, 1998b). Likewise, gravity sensing in the moss protonema is restricted to the growing tip cells where starch-rich plastids trigger re-orientation of the cytoskeleton to initiate curvature of the growing cell (Blancaflor, 2002; Sack et al., 2001; Schwuchow et al., 2002). Thus, both abnormalities argue in favor of a defective cytoskeleton in the  $\Delta ftsZ3$  mutants, albeit a putative integration of ancient tubulin FtsZ3 into the classical cytoskeleton of *Physcomitrella* remains to be elucidated.

Up to now, *ftsZ3* genes have only been identified in the moss *P. patens* and in the lycophyte *Selaginella moellendorffii*, while flowering plants only encode FtsZ proteins of the FtsZ subfamilies 1 and 2. While PpftsZ1- and PpftsZ2-genes possess six introns, the PpftsZ3 gene possesses only three introns. This 'more ancient' gene structure of PpftsZ3 and the importance of its protein for cellular functions reveal its close relationship to its bacterial ancestor. As FtsZ3 not only is dually targeted to plastids and to the cytosol of *P. patens*, but also exerts specific functions in both compartments, it integrates the FtsZ1/FtsZ2-based plastoskeleton with the cytoskeleton in this species.

Although we here found several FtsZ functions to be similar between *P. patens* and *A. thaliana*, there were also striking differences. Given the about 450 million years of separate evolution between both plant species and the basal position mosses retained in land plant evolution (Lang et al., 2008), it is plausible that the chloroplast division apparatus of mosses has retained more bacterial features than those of seed plants. Thus, our results are in good accordance with the elegant works of Machida et al. (2006) and Garcia et al. (2008) demonstrating the importance of homologs of the bacterial Pbp and MurE for plastid division in *P. patens* (reviewed in Reski, 2009).

Besides that, an involvement of the 'bacterial tubulin' FtsZ3 in cellular functions may have resulted in a moss-specific evolution of eukaryotic  $\beta$ -tubulins as described for *P. patens* by

Jost et al. (2004). Thus, the *ftsZ* gene family may not only serve as a model to study post-duplication evolution and the impact of redundancy, sub- and neofunctionalization, but may also be instructive to understand the evolution of the cytoskeleton in land plants.

## METHODS

### Plant Material and Growth Conditions

*P. patens* was cultured as described in Strepp et al. (1998).

For the adjustment of dry weight in *P. patens*, 10 mL of liquid culture were removed prior to sub-culturing and filtered through gauze (Miracloth, Calbiochem, Schwalbach, Germany). The dry weight was determined after drying the sample for 2 h at 105°C.

Knockout mutants described in this study are deposited in the International Moss Stock Center with the accessions IMSC 40128–40149 ( $\Delta ftsZ1-1$  (#216),  $\Delta ftsZ1-2$  (#12, #14, #Q1),  $\Delta ftsZ1-1/1-2$  (#12, #14, #15, #45, #46),  $\Delta ftsZ3$  (#12, #32, #38, #61, #114),  $\Delta ftsZ2-1$ ,  $\Delta ftsZ2-2$  (#34, #97, #101, #103, #134),  $\Delta ftsZ2-1/2-2$  (#8, #23). Mutant numbers as shown in text and figures are indicated in brackets.

### Phenotypic Analysis

To investigate the development of negatively gravitropic, dark-grown caulonema filaments, 5  $\mu$ L droplets from liquid cultures with a dry weight of 100 mg L<sup>-1</sup> were placed on solid Knop medium. Plates were sealed and placed in a climate chamber with standard conditions for 6 d. Subsequently, the plates were wrapped in tin foil and positioned vertically. Culturing under standard conditions was carried out for another 7 d. Single protonema colonies were examined with regard to the development of caulonema filaments. Pictures of representative colonies were taken.

For the determination of gametophore, leaf and cell dimensions as well as cell wall thickness, the LSM 5 image browser (Zeiss, Jena, Germany) was employed. Raw data were analyzed in Excel. Statistical evaluation was performed using SigmaPlot 9.0 (Systat Software GmbH, Erkrath, Germany). Statistical evaluation of the results was done via *t*-test. *P*-values smaller than 0.001 indicate significant differences between the two groups tested.

### Knockout Constructs and Plant Transformation

For generation of knockout constructs, genomic fragments of the *ftsZ* genes were amplified from *P. patens* genomic DNA, cloned into pCHR4-TOPO (Invitrogen, Karlsruhe, Germany) and selection cassettes were inserted into the linearized vectors (for details, see Table 2).

Protoplast isolation from *P. patens* protonema, transformation, and regeneration of stably transformed plants were performed as described previously (Strepp et al., 1998).

For the generation of *ftsZ1-1/1-2* double knockouts, a  $\Delta ftsZ1-1$  mutant was transformed with the knockout construct for *ftsZ1-2*. For the generation of *ftsZ2-1/2-2* double

**Table 2.** Primers for the Amplification of Genomic *ftsZ* Fragments Are Given as Pairs.

Knockout construct	Oligonucleotides (5'-3')	Selection cassette (insertion sites)
<i>ftsZ1-1</i>	fwd: CTGCAGAAGTGGCGTGTGAAG rev: AGGCATCCGTCATCCCAGAATTC	nptII ( <i>Clal-SalI</i> )
<i>ftsZ1-2</i>	fwd: ATGGGCTCTACGGCGAGGTT rev: GAGGCAGCCTGAATTGCAGCT	hpt ( <i>HpaI-EcoRV</i> )
<i>ftsZ3</i>	fwd: ATGATCACGTGTAGGGTTGG rev: CGATGTTGACCTCGTGAAGAG	nptII ( <i>AgeI-HpaI</i> )
<i>ftsZ2-2</i>	fwd: CAGGGTGAGCTCGCGAGTG rev: TTTGGTACCCTGATGAAATCAAACTAATACCAC	hpt ( <i>HindIII-BamHI</i> )

Restriction sites flanking the selection cassettes are listed in brackets. nptII (neomycin phosphotransferase II) was amplified from pRT101neo (R. Strepp); hpt (hygromycin phosphotransferase) was amplified from pCAMBIA1305 (Huether et al., 2005).

knockouts, the already existing  $\Delta$ *ftsZ2-1* mutant was transformed with the knockout construct for *ftsZ2-2*.

### Plant Screening

Plants were screened for disruption of the respective *ftsZ* locus and correct 5' and 3' integration of the knockout construct via direct PCR (Supplemental Figure 1) (Schween et al., 2002). Primers used for the analysis are listed in Table 3.

### RT-PCR

After RNA-isolation using Trizol reagent (Invitrogen, Karlsruhe, Germany) and cDNA synthesis from 2  $\mu$ g total RNA using Superscript III Reverse Transcriptase (Invitrogen, Karlsruhe, Germany), RT-PCR was performed to show the absence of the respective *ftsZ* transcript in the knockout plants. Primers used for the analysis are listed in Table 4. Primers for the constitutively expressed ribosomal gene *121* were used as control.

### Quantitative Real-Time PCR

For qRT-PCR analysis, RNA was extracted using Trizol reagent (Invitrogen, Karlsruhe, Germany) and purified using RNeasy columns (Qiagen, Hilden, Germany). An additional DNase I (Fermentas, St Leon-Rot, Germany) digestion was performed after RNA cleanup. Samples were reverse-transcribed into first-strand cDNA using Taq Man Reverse Transcription Reagents (Applied Biosystems, Darmstadt, Germany). Then, PCR was carried out using gene-specific primers (Table 5) and LightCycler® 480 SYBR Green I Master (Roche, Mannheim, Germany) with a Roche 480 Light Cycler following the manufacturer's instructions. *EF1 $\alpha$*  and *L21* were used as reference genes to normalize for variation in the amount of cDNA template. Each real-time PCR experiment contained three technical replicates using 50 ng of cDNA in a total volume of 20  $\mu$ l. Melting curve analysis for validation of the PCR reaction was carried out routinely. *FtsZ* expression levels were calculated relative to wild-type transcript abundance employing relative quantification with efficiency correction (Livak and Schmittgen, 2001; Rasmussen, 2001).

**Table 3.** Primers for PCR Screens of Putative *ftsZ* Knockout Plants.

Gene	Screen	Oligonucleotides (5'-3')
<i>ftsZ1-1</i>	WT	fwd: ATCGCGTTCAAATCGGCGAAG rev: CTTTCAAGCCTGGGCTTAACCA
	5'	fwd: AGACGGTTTGTAGATGGCG rev: TGTCGTGCTCCACCATGTT
	3'	fwd: GTTGAGCATATAAGAAAC rev: CTGTTACAATCTGCATCA
<i>ftsZ1-2</i>	WT	fwd: GCGTCGGCAGGCTGTGTAT rev: CGCGATGTTGGCTTGTG
	5'	fwd: GCGTAGCCTTTCAGTAC rev: ATAGTGACCTTAGGCGAC
	3'	fwd: TTAACATGTAATGCATGACG rev: CTGAGATACAGTATCACTTC
<i>ftsZ3</i>	WT	fwd: TTGGACAGGACACGACGCCGCC rev: GCTCCTGAACCAGTACCGCCACC
	5'	fwd: AACCTTGTGGACGACTGTG rev: TGTCGTGCTCCACCATGTT
	3'	fwd: GTTGAGCATATAAGAAACCC rev: CCAGCTTTGAGTACAGGCTT
<i>ftsZ2-2</i>	5'	fwd: ATGGCGCTGTAGGCGAGTC rev: ATAGTGACCTTAGGCGAC
	3'	fwd: TTAACATGTAATGCATGACG rev: TCATTAAGTCTGCCACTCC

WT: PCR product can only be synthesized in the wild-type due to primer binding either in a deleted region or flanking the selection cassette, thus yielding a large product that cannot be amplified. 5' and 3': primer pairs bind outside the knockout construct and inside the selection cassette, thus proving correct integration at the genomic locus.

ANOVA of wild-type transcript levels in protonemata was performed using the functions *aov*, *lm*, *anova*, and *TukeyHSD* implemented in R 2.4.1 (The R Development Core Team, 2009). Significance was inferred assuming a 99% confidence interval.

**Table 4.** Primers for RT-PCR Analysis of Putative *ftsZ* Knockout Plants.

Gene	Oligonucleotides (5'-3')
<i>ftsZ1-1</i>	fwd: ATGATGAGCTCCATGGTGAG rev: TCAGACACGGTGTGACTTC
<i>ftsZ1-2</i>	fwd: ATGGGCTCTACGGCGAGGTT rev: GAGGCAGCTGAATTGCAGCT
<i>ftsZ3</i>	fwd: TTGGACAGGACACGACAGCCGGC rev: CAGTGTACGCCGATGGCGCATG
<i>ftsZ2-2</i>	fwd: TCATTGCTGGTGTAGCGAA rev: ATCGTAGAGCTATTGCCAC
L21	fwd: GGTTGGTCATGGGTTGCG rev: GAGGTCAACTGTCTCGCC

**Table 5.** Primers for qRT-PCR Analysis of *ftsZ* Transcript Abundance in Wild-Type and *ftsZ* Single and Double Knockout Plants.

Gene	Oligonucleotides (5'-3')
<i>ftsZ1-1</i>	fwd: CGTTTCTAGGTCGGAGAGGC rev: ACGAAATCTTGATGAGGTGGG
<i>ftsZ1-2</i>	fwd: ATGGGCTCTACGGCGAGGTT rev: TACCGAGCCTACTCTCCGCTC
<i>ftsZ3</i>	fwd: GAGCTTTCGATGGCACTTGA rev: TTGTGAGCTCGGGTGAAC
<i>ftsZ2-1</i>	fwd: GTTGTTAGTGGGTGCTCGG rev: GGGGTTACATCGCAAAGG
<i>ftsZ2-2</i>	fwd: TGCCATTAGTCTCCATTGT rev: TTGCATACTGCATACTCCGTG
<i>EF1<math>\alpha</math></i>	fwd: CGACGCCCTGGACATC rev: CCTGCGAGGTTCCCGTAA
L21	fwd: GGTTGGTCATGGGTTGCG rev: GACCTCAACTGTCTCGCC

### Northern Blotting

RNA blot hybridization was carried out as described (Frank et al., 2005) with a radioactively labeled *ftsZ2-2* cDNA probe that was amplified using the primers 5'-AAGGTAGTACAAATGGGATGGC-3' and 5'-TCATTAAGTCTGCCACTCCAC-3'.

### Microscopic Observations

Bright-field images of cells were taken with a charge-coupled device (CCD) camera (AxioCam MRc5 or ICc1, Zeiss, Jena, Germany) under microscope Axioplan and Stemi 2000C (Zeiss, Jena, Germany). Electron microscopy of protonema cells was carried out at the CM 10 (Philips, Hamburg, Germany) at 60 kV.

### Accession Numbers

Sequence data from this article can be found in the GenBank data libraries under accession numbers as follows: *FtsZ1-1* XM\_001780186 (Phypa\_196781); *FtsZ2-1* XM\_001765901 (Phypa\_212480); *FtsZ3* XM\_001765160 (Phypa\_211907); *FtsZ2-2* XM\_001766723 (Phypa\_185873); *FtsZ1-2* XM\_001769006 (Phypa\_187670). *P. patens* gene models are given in brackets.

## SUPPLEMENTARY DATA

Supplementary Data are available at *Molecular Plant Online*.

### FUNDING

This work was supported by the Deutsche Forschungsgemeinschaft (SFB388 and Re837/10) and by the Excellence Initiative of the German Federal and State Governments (GSC-4 and EXC 294).

## ACKNOWLEDGMENTS

We thank Ida Suppanz for designing parts of the *ftsZ1-1* knockout construct and Eva L. Decker and Agnes Novakovic for planning the *ftsZ2-2* construct and doing the cloning, respectively. We are also grateful to Justine Kiessling for creating the *ftsZ3* construct and to Volker Speth for his help with TEM and during the preparation of specimens. No conflict of interest declared.

## REFERENCES

- Aaron, M., Charbon, G., Lam, H., Schwarz, H., Vollmer, W., and Jacobs-Wagner, C. (2007). The tubulin homologue FtsZ contributes to cell elongation by guiding cell wall precursor synthesis in *Caulobacter crescentus*. *Mol. Microbiol.* **64**, 938–952.
- Allard, J.F., and Cytrynbaum, E.N. (2009). Force generation by a dynamic Z-ring in *Escherichia coli* cell division. *Proc. Natl Acad. Sci. U S A.* **106**, 145–150.
- Bierfreund, N.M., Reski, R., and Decker, E.L. (2003). Use of an inducible reporter gene system for the analysis of auxin distribution in the moss *Physcomitrella patens*. *Plant Cell Rep.* **21**, 1143–1152.
- Blancaflor, E.B. (2002). The cytoskeleton and gravitropism in higher plants. *J. Plant Growth Regul.* **21**, 120–136.
- Chen, T., Teng, N., Wu, X., Wang, Y., Tang, W., Samaj, J., Baluska, F., and Lin, J. (2007). Disruption of actin filaments by latrunculin B affects cell wall construction in *Picea meyeri* pollen tube by disturbing vesicle trafficking. *Plant Cell Physiol.* **48**, 19–30.
- Cole, R.A., and Fowler, J.E. (2006). Polarized growth: maintaining focus on the tip. *Curr. Opin. Plant Biol.* **9**, 579–588.
- Cove, D.J. (1992). Chapter 12: Regulation of development in the moss, *Physcomitrella patens*. In *Development: The Molecular Genetic Approach*, Russo, V.E.A., Brody, S., Cove, D., Ottolenghi, S., eds (Berlin: Springer-Verlag).
- Dai, K., and Lutkenhaus, J. (1991). *ftsZ* is an essential cell division gene in *Escherichia coli*. *J. Bacteriol.* **173**, 3500–3506.
- de Boer, P., Crossley, R., and Rothfield, L. (1992). The essential bacterial cell-division protein FtsZ is a GTPase. *Nature.* **359**, 254–256.

- Decker, E.L., Frank, W., Sarnighausen, E., and Reski, R. (2006). Moss systems biology en route: phytohormones in *Physcomitrella* development. *Plant Biol. (Stuttg.)*, **8**, 397–405.
- El-Kafafi, S., Mukherjee, S., El-Shami, M., Putaux, J.L., Block, M.A., Pignot-Paintrand, I., Lerbs-Mache, S., and Falconet, D. (2005). The plastid division proteins, FtsZ1 and FtsZ2, differ in their biochemical properties and sub-plastidial localization. *Biochem J.* **387**, 669–676.
- El-Shami, M., El-Kafafi, S., Falconet, D., and Lerbs-Mache, S. (2002). Cell cycle-dependent modulation of FtsZ expression in synchronized tobacco BY2 cells. *Mol. Genet. Genomics*, **267**, 254–261.
- Erickson, H.P., Taylor, D.W., Taylor, K.A., and Bramhill, D. (1996). Bacterial cell division protein FtsZ assembles into protofilament sheets and minirings, structural homologs of tubulin polymers. *Proc. Natl Acad. Sci. U S A.* **93**, 519–523.
- Frank, W., Ratnadewi, D., and Reski, R. (2005). *Physcomitrella patens* is highly tolerant against drought, salt and osmotic stress. *Planta*, **220**, 384–394.
- Garcia, M., Myouga, F., Takechi, K., Sato, H., Nabeshima, K., Nagata, N., Takio, S., Shinozaki, K., and Takano, H. (2008). An *Arabidopsis* homolog of the bacterial peptidoglycan synthesis enzyme MurE has an essential role in chloroplast development. *Plant J.* **53**, 924–934.
- Gilson, P.R., and Beech, P.L. (2001). Cell division protein FtsZ: running rings around bacteria, chloroplasts and mitochondria. *Res. Microbiol.* **152**, 3–10.
- Gould, S.B., Waller, R.F., and McFadden, G.I. (2008). Plastid evolution. *Annu. Rev. Plant Biol.* **59**, 491–517.
- Gray, M.W. (1992). The endosymbiont hypothesis revisited. *Int. Rev. Cytol.* **141**, 233–357.
- Gremillon, L., Kiessling, J., Hause, B., Decker, E.L., Reski, R., and Sarnighausen, E. (2007). Filamentous temperature-sensitive Z (FtsZ) isoforms specifically interact in the chloroplasts and in the cytosol of *Physcomitrella patens*. *New Phytologist*, **176**, 299–310.
- Haney, S.A., Glasfeld, E., Hale, C., Keeney, D., He, Z., and de Boer, P. (2001). Genetic analysis of the *Escherichia coli* FtsZ.ZipA interaction in the yeast two-hybrid system: characterization of FtsZ residues essential for the interactions with ZipA and with FtsA. *J. Biol. Chem.* **276**, 11980–11987.
- Harrison, C.J., Roeder, A.H.K., Meyerowitz, E.M., and Langdale, J.A. (2009). Local cues and asymmetric cell divisions underpin body plan transitions in the moss *Physcomitrella patens*. *Curr. Biol.* **19**, 461–471.
- Huether, C.M., Lienhart, O., Baur, A., Stemmer, C., Gorr, G., Reski, R., and Decker, E.L. (2005). Glyco-engineering of moss lacking plant-specific sugar residues. *Plant Biol. (Stuttg.)*, **7**, 292–299.
- Hussey, P.J., Ketelaar, T., and Deeks, M.J. (2006). Control of the actin cytoskeleton in plant cell growth. *Annu. Rev. Plant Biol.* **57**, 109–125.
- Jeong, W.J., Park, Y.I., Suh, K., Raven, J.A., Yoo, O.J., and Liu, J.R. (2002). A large population of small chloroplasts in tobacco leaf cells allows more effective chloroplast movement than a few enlarged chloroplasts. *Plant Physiol.* **129**, 112–121.
- Jost, W., Baur, A., Nick, P., Reski, R., and Gorr, G. (2004). A large plant beta-tubulin family with minimal C-terminal variation but differences in expression. *Gene*, **340**, 151–160.
- Kasten, B., and Reski, R. (1997).  $\beta$ -lactam antibiotics inhibit chloroplast division in a moss (*Physcomitrella patens*) but not in tomato (*Lycopersicon esculentum*). *J. Plant Physiol.* **150**, 137–140.
- Kiessling, J., Kruse, S., Rensing, S.A., Harter, K., Decker, E.L., and Reski, R. (2000). Visualization of a cytoskeleton-like FtsZ network in chloroplasts. *J. Cell Biol.* **151**, 945–950.
- Kiessling, J., Martin, A., Gremillon, L., Rensing, S.A., Nick, P., Sarnighausen, E., Decker, E.L., and Reski, R. (2004). Dual targeting of plastid division protein FtsZ to chloroplasts and the cytoplasm. *EMBO Rep.* **5**, 889–894.
- Köhler, R.H., Cao, J., Zipfel, W.R., Webb, W.W., and Hanson, M.R. (1997). Exchange of protein molecules through connections between higher plant plastids. *Science*, **276**, 2039–2042.
- Kuroiwa, T., Kuroiwa, H., Sakai, A., Takahashi, H., Toda, K., and Itoh, R. (1998). The division apparatus of plastids and mitochondria. *Int. Rev. Cytol.* **181**, 1–41.
- Kuroiwa, T., Misumi, O., Nishida, K., Yagisawa, F., Yoshida, Y., Fujiwara, T., and Kuroiwa, H. (2008). Vesicle, mitochondrial, and plastid division machineries with emphasis on dynamin and electron-dense rings. *Int. Rev. Cell Mol. Biol.* **271**, 97–152.
- Lang, D., Zimmer, A.D., Rensing, S.A., and Reski, R. (2008). Exploring plant biodiversity: the *Physcomitrella* genome and beyond. *Trends Plant Sci.* **13**, 542–549.
- Larkin, J.C., Brown, M.L., and Schiefelbein, J. (2003). How do cells know what they want to be when they grow up? Lessons from epidermal patterning in *Arabidopsis*. *Annu. Rev. Plant Biol.* **54**, 403–430.
- Livak, K.J., and Schmittgen, T.D. (2001). Analysis of relative gene expression data using real-time quantitative PCR and the 2(-Delta Delta C(T)) method. *Methods*, **25**, 402–408.
- Lowe, J., and Amos, L.A. (1998). Crystal structure of the bacterial cell-division protein FtsZ. *Nature*, **391**, 203–206.
- Ma, X., and Margolin, W. (1999). Genetic and functional analyses of the conserved C-terminal core domain of *Escherichia coli* FtsZ. *J. Bacteriol.* **181**, 7531–7544.
- Machida, M., et al. (2006). Genes for the peptidoglycan synthesis pathway are essential for chloroplast division in moss. *Proc. Natl Acad. Sci. U S A.* **103**, 6753–6758.
- Maple, J., Aldridge, C., and Moller, S.G. (2005). Plastid division is mediated by combinatorial assembly of plastid division proteins. *Plant J.* **43**, 811–823.
- Martin, A., Lang, D., Heckmann, J., Zimmer, A.D., Vervliet-Scheebaum, M., and Reski, R. (2009). A uniquely high number of ftsZ genes in the moss *Physcomitrella patens*. *Plant Biology*, **11**, 744–750.
- Martin, W., Stoebe, B., Goremykin, V., Hapsmann, S., Hasegawa, M., and Kowallik, K.V. (1998). Gene transfer to the nucleus and the evolution of chloroplasts. *Nature*, **393**, 162–165.
- McAndrew, R.S., Froehlich, J.E., Vitha, S., Stokes, K.D., and Osteryoung, K.W. (2001). Colocalization of plastid division proteins in the chloroplast stromal compartments establishes a new functional relationship between FtsZ1 and FtsZ2 in higher plants. *Plant Phys.* **127**, 1656–1666.
- McAndrew, R.S., Olson, B.J., Kadirjan-Kalbach, D.K., Chi-Ham, C.L., Vitha, S., Froehlich, J.E., and Osteryoung, K.W. (2008). *In vivo*

- quantitative relationship between plastid division proteins FtsZ1 and FtsZ2 and identification of ARC6 and ARC3 in a native FtsZ complex. *Biochem. J.* **412**, 367–378.
- Menand, B., Calder, G., and Dolan, L. (2007). Both chloronemal and caulonemal cells expand by tip growth in the moss *Physcomitrella patens*. *J. Exp. Bot.* **58**, 1843–1849.
- Miyagishima, S.Y., Froehlich, J.E., and Osteryoung, K.W. (2006). PDV1 and PDV2 mediate recruitment of the dynamin-related protein ARC5 to the plastid division site. *Plant Cell.* **18**, 2517–2530.
- Miyagishima, S.Y., Kuwayama, H., Urushihara, H., and Nakanishi, H. (2008). Evolutionary linkage between eukaryotic cytokinesis and chloroplast division by dynamin proteins. *Proc. Natl Acad. Sci. U S A.* **105**, 15202–15207.
- Osawa, M., Anderson, D.E., and Erickson, H.P. (2008). Reconstitution of contractile FtsZ rings in liposomes. *Science.* **320**, 792–794.
- Osteryoung, K.W., and Vierling, E. (1995). Conserved cell and organelle division. *Nature.* **376**, 473–474.
- Osteryoung, K.W., Stokes, K.D., Rutherford, S.M., Percival, A.L., and Lee, W.Y. (1998). Chloroplast division in higher plants requires members of two functionally divergent gene families with homology to bacterial *ftsZ*. *Plant Cell.* **10**, 1991–2004.
- Paredes, A.R., Somerville, C.R., and Ehrhardt, D.W. (2006). Visualization of cellulose synthase demonstrates functional association with microtubules. *Science.* **312**, 1491–1495.
- Possingham, J.V., and Lawrence, M.E. (1983). Controls to plastid division. *Int. Rev. Cytol.* **84**, 1–56.
- Rasmussen, R. (2001). Quantification on the LightCycler instrument. In *Rapid Cycle Real-Time PCR: Methods and Applications*, Meuer, S., Wittwer, C., Nakagawara, K., eds (Heidelberg: Springer).
- Rensing, S.A., et al. (2008). The *Physcomitrella* genome reveals evolutionary insights into the conquest of land by plants. *Science.* **319**, 64–69.
- Rensing, S.A., Ick, J., Fawcett, J.A., Lang, D., Zimmer, A., Van de Peer, Y., and Reski, R. (2007). An ancient genome duplication contributed to the abundance of metabolic genes in the moss *Physcomitrella patens*. *BMC Evol. Biol.* **7**, 130.
- Rensing, S.A., Kiessling, J., Reski, R., and Decker, E.L. (2004). Diversification of *ftsZ* during early land plant evolution. *J. Mol. Evol.* **58**, 154–162.
- Reski, R. (1998a). *Physcomitrella* and *Arabidopsis*: the David and Goliath of reverse genetics. *Trends Plant Sci.* **3**, 209–210.
- Reski, R. (1998b). Development, genetics and molecular biology of mosses. *Botanica Acta.* **111**, 1–15.
- Reski, R. (2002). Rings and networks: the amazing complexity of FtsZ in chloroplasts. *Trends Plant Sci.* **7**, 103–105.
- Reski, R. (2009). Challenges to our current view on chloroplasts. *Biological Chemistry.* **390**, 731–738.
- Sack, F.D., Schwuchow, J.M., Wagner, T., and Kern, V. (2001). Gravity sensing in moss protonemata. *Adv. Space Res.* **27**, 871–876.
- Schween, G., Fleig, S., and Reski, R. (2002). High-throughput-PCR screen of 15,000 transgenic *Physcomitrella* plants. *Plant Mol. Biol. Rep.* **20**, 43–47.
- Schwuchow, J.M., Kern, V.D., White, N.J., and Sack, F.D. (2002). Conservation of the plastid sedimentation zone in all moss genera with known gravitropic protonemata. *J. Plant Growth Regul.* **21**, 146–155.
- Shibaoka, H., and Nagai, R. (1994). The plant cytoskeleton. *Curr. Opin. Cell Biol.* **6**, 10–15.
- Smith, L.G., and Oppenheimer, D.G. (2005). Spatial control of cell expansion by the plant cytoskeleton. *Annu. Rev. Cell Dev. Biol.* **21**, 271–295.
- Stokes, K.D., McAndrew, R.S., Figueroa, R., Vitha, S., and Osteryoung, K.W. (2000). Chloroplast division and morphology are differentially affected by overexpression of FtsZ1 and FtsZ2 genes in *Arabidopsis*. *Plant Physiol.* **124**, 1668–1677.
- Strepp, R., Scholz, S., Kruse, S., Speth, V., and Reski, R. (1998). Plant nuclear gene knockout reveals a role in plastid division for the homolog of the bacterial cell division protein FtsZ, an ancestral tubulin. *Proc. Natl Acad. Sci. U S A.* **95**, 4368–4373.
- Suppanz, I., Sarnighausen, E., and Reski, R. (2007). An integrated physiological and genetic approach to the dynamics of FtsZ targeting and organisation in a moss, *Physcomitrella patens*. *Protoplasma.* **232**, 1–9.
- The R Development Core Team (2009). A Language and Environment for Statistical Computing. V2.4.1. ISSN 3-900051-07-0.
- Vandenbussche, F., Fierro, A.C., Wiedemann, G., Reski, R., and Van Der Straeten, D. (2007). Evolutionary conservation of plant gibberellin signalling pathway components. *BMC Plant Biol.* **7**, 65.
- Vandesompele, J., De Preter, K., Pattyn, F., Poppe, B., Van Roy, N., De Paepe, A., and Speleman, F. (2002). Accurate normalization of real-time quantitative RT-PCR data by geometric averaging of multiple internal control genes. *Genome Biol.* **3**, RESEARCH0034.
- Varma, A., de Pedro, M., and Young, K.D. (2007). FtsZ directs a second mode of peptidoglycan synthesis in *Escherichia coli*. *J. Bacteriol.* **189**, 5692–5704.
- Vitha, S., Froehlich, J.E., Koksharova, O., Pyke, K.A., van Erp, H., and Osteryoung, K.W. (2003). ARC6 is a J-domain plastid division protein and an evolutionary descendant of the cyanobacterial cell division protein Ftn2. *Plant Cell.* **15**, 1918–1933.
- Vitha, S., McAndrew, R.S., and Osteryoung, K.W. (2001). FtsZ ring formation at the chloroplast division site in plants. *J. Cell Biol.* **153**, 111–120.
- Yan, K., Pearce, K.H., and Payne, D.J. (2000). A conserved residue at the extreme C-terminus of FtsZ is critical for the FtsA–FtsZ interaction in *Staphylococcus aureus*. *Biochem. Biophys. Res. Commun.* **270**, 387–392.
- Yoshida, Y., Kuroiwa, H., Misumi, O., Nishida, K., Yagisawa, F., Fujiwara, T., Nanamiya, H., Kawamura, F., and Kuroiwa, T. (2006). Isolated chloroplast division machinery can actively constrict after stretching. *Science.* **313**, 1435–1438.